ISPRS Annals of the Photogrammetry, Remote Sensing and Spatial Information Sciences, Volume X-5/W2-2025
Unleashing the power of Geospatial & Frontier Technologies for a Sustainable Future – GIFTS Summit 2025,
1–3 September 2025, Symbiosis International University, Pune, India

From Maps to Action: Using Geospatial Insights to Enable Community Greening for Urban Resilience in Pune

Harsh Desai[1], Shamita Kumar[2*]

[1,2] Bharati Vidyapeeth Deemed University, Institute of Environment Education and Research, Pune, 411043, INDIA,
[*]Corresponding author

KEYWORDS: Urban Heat Island (UHI); Heat Mitigation Index (HMI); InVEST Urban Cooling Model; Green infrastructure; Citizen engagement; Cooling Capacity in cities

ABSTRACT

The rapid urbanization of Pune, Maharashtra, over recent decades has intensified thermal impacts through the Urban Heat Island (UHI) effect, caused by replacing natural surfaces with impervious concrete and asphalt. This has led to higher nighttime land surface temperatures (LST), particularly in builtup and periurban areas compared to rural surroundings. While traditional UHI assessments correlate LST with land use alone, the InVEST Urban Cooling Model integrates remotely sensed biophysical parameters such as albedo, shading, evapotranspiration, along with proximity to green infrastructure into a pixel level framework that calculates Cooling Capacity (CC) and a Heat Mitigation Index (HMI). Seasonal LST composites for summer, monsoon, and winter were generated from Landsat 8 thermal bands (cloud cover <10 using the InVEST model). Per pixel Cooling Capacity values ranged from 0.116 to 0.943, while HMI values spanned from 0.116 to 0.943 across the metropolitan region. The highest values (>0.70) were found in heavily vegetated wards with dense forest cover and riverine zones, while the lowest values (<0.35) occurred in industrial and high density built-up areas with minimal vegetation cover. The resulting decision-ready maps provide a spatial blueprint not only for urban planners and local authorities but also for citizen groups, neighbourhood associations, and NGOs to collaboratively identify and prioritise greening interventions. By combining geospatial evidence with participatory planning, the study fosters community-led initiatives- such as urban forests, green roofs, and vegetative corridors- that are locally relevant, socially inclusive, and climate-resilient. This approach empowers citizens to be active co-creators of cooler, healthier, and more liveable urban environments across Pune's urban- rural continuum.

1. INTRODUCTION

Urban Heat Islands (UHI) are among the most pressing environmental challenges in rapidly urbanizing regions. They are a well documented phenomenon characterized by elevated temperatures in urban areas relative to their rural surroundings, driven primarily by the replacement of natural land cover with impervious surfaces such as asphalt and concrete (Favazza et al., 2022). The intensification of UHI has been linked to both rapid urbanization and climate change leading to increased energy consumption, deteriorated air quality, and public health risks (Weng, 2020). The study of UHIs has expanded considerably over the past two decades, with advances in remote sensing, geospatial modelling, and urban climate analysis enabling increasingly detailed and spatially explicit assessments (Soto et al., 2023a).

Thermal remote sensing forms the backbone of most UHI analyses, with platforms such as Landsat, MODIS, and Sentinel providing critical Land Surface Temperature (LST) data (Favazza et al., 2022; Kasniza Jumari et al., 2023). LST retrieval from thermal infrared imagery enables the mapping of spatial temperature gradients, with studies reporting increases of 2-3°C over decadal timescales in rapidly growing cities (Saini et al., 2025). While some investigations employ simple LST-LULC correlations, more advanced approaches integrate multi-temporal and multi-sensor datasets (Cecinati et al., 2019; Li et al., 2024) and leverage object-based image analysis for automated hotspot extraction (Weng, 2020). Machine learning methods, including support vector machines optimized with particle swarm algorithms, have demonstrated high predictive accuracy with coefficients of determination up to 0.892 and RMSE as low as 0.42°C.

Recent methodological developments have emphasized multi-scale assessment frameworks, such as the integration of Local Climate Zone (LCZ) classification with thermal mapping, acknowledging that UHI intensity varies with urban morphology and land use (Isinkaralar et al., 2025; Fung et al., 2022). The influence of biophysical parameters- including albedo, vegetation shading, and evapo-transpiration, has been shown to be substantial in shaping microclimates (Korotczuk-Zych, 2023; Bosch and Hamel, 2021). Vegetation indices such as NDVI typically show negative correlations with LST, while built-up indices like NDBI show positive correlations (Duan et al., 2025), with studies reporting strong relationships between vegetation cover and cooling (Hasan, 2024). Urban form parameters such as the sky view factor (SVF) and building density also significantly influence cooling effectiveness (Korotczuk-Zych, 2023).

Global evidence highlights the capacity of urban green spaces to lower LST by up to 4.73°C when coverage is increased and spatial distribution is optimized (Xu et al., 2024). Planned cities with higher vegetation coverage show markedly lower LSTs compared to unplanned urban areas, which often experience expansion of high LST zones exceeding 35°C (Ullah et al., 2025). Temporal and spatial variability is pronounced. For example, in Chennai, India, UHI intensity increased by 450% over 14 years, driven largely by urban expansion and seasonal variations in climate (Cecinati et al., 2019).

Among the ecosystem service modelling approaches for UHI mitigation, the InVEST Urban Cooling Model has emerged as a robust and flexible tool, estimating temperature reductions based on shading, evapotranspiration, albedo, and building density (Bosch and Hamel, 2021; Hamel et al., 2024). Its ability to operate in both data rich and data scarce contexts makes it suitable for developing countries (Hamel and Bosch, 2023). Validation studies have shown strong correlations with air temperature observations, particularly at night (Hamel et al., 2024), and applications in cities from Paris to Rajshahi have confirmed its relevance across diverse urban morphologies (Hasan, 2024). Studies in Bangladesh, for instance, reported that every 0.1 unit increase in Heat Mitigation Index (HMI) corresponded to a 0.53°C decrease in LST (Hasan, 2024). In India, applications have been limited to smaller scale studies, such as a scenario analysis in Nagpur estimating 21-29% potential energy savings from strategic greening (Kadaverugu and Sharma, 2021).

Despite methodological advances, several gaps remain. Many studies are constrained by the coarse spatial resolution of satellite thermal sensors (Tonekaboni, 2023), limited ground validation (Parlow, 2021), seasonal bias in datasets (Cecinati et al., 2019), and insufficient integration of social vulnerability into UHI frameworks (Elmarakby and Elkadi, 2024; Li et al., 2024). In India, metropolitan scale assessments are scarce, and few have incorporated the unique climatic influences of monsoons, dust storms, or high humidity into UHI modelling (Ullah et al., 2025). Even fewer studies have linked UHI mitigation modelling to citizen led greening initiatives, despite emerging evidence from global contexts that participatory planning can enhance both effectiveness and public acceptance of interventions (Zardo et al., 2017).

The Pune Metropolitan Region presents an ideal setting to address some of these gaps. As one of India's fastest growing metropolitan areas, it combines a dense urban core, rapidly developing periurban zones, and surrounding agricultural landscapes, alongside active environmental organizations and citizen groups engaged in greening. This study applies the InVEST Urban Cooling Model at a metropolitan scale to quantify seasonal variations in Cooling Capacity and HMI, identify priority greening zones, and link these outputs to actionable pathways for community led climate resilience. In doing so, it advances both the scientific application of geospatial modelling for UHI mitigation in India and the integration of participatory approaches into metropolitan scale climate adaptation. The remainder of this paper is structured as follows: Section 2 describes the study area and datasets; Section 3 outlines the methodology, including LST derivation, model parameterization, and spatial analysis; Section 4 presents the results; Section 5 discusses their implications for urban resilience and community engagement; and Section 6 concludes with key findings and recommendations.

2. STUDY AREA AND DATA

2.1 Study Area

Figure 1. Pune Metropolitan Region - the study area

The Pune Metropolitan Region (PMR) is located between 18°25′-19°20′ N latitude and 73°10′-74°15′ E longitude in western Maharashtra, India, covering approximately 7,256 km² (Figure 1). It encompasses the Pune and Pimpri-Chinchwad municipal corporations, several municipal councils, census towns, and rural hinterlands. The region's population exceeds 7 million, making it one of the fastest-growing metropolitan areas in the country. Topographically, the PMR consists of undulating hills, plateau regions, and river valleys, with elevations ranging from ~530 m in the plains to >900 m in the surrounding hill ranges. The Mula and Mutha rivers traverse the urban core, influencing microclimatic conditions.

The PMR experiences a tropical wet and dry climate with three distinct seasons: summer (March-May), monsoon (June-September), and winter (October-February). Maximum summer temperatures frequently exceed 37°C, while winter temperatures can drop to ~10°C. Annual rainfall averages 700-800 mm, concentrated in the monsoon season. Vegetation cover is highest in periurban and rural areas, while urban greenery is largely confined to parks, institutional campuses, and roadside plantations. Over the past three decades, rapid land use conversion from agriculture and open spaces to built up areas has intensified the Urban Heat Island (UHI) effect.

2.2 Data Sources

Satellite Data: Landsat 8 Operational Land Imager (OLI) and Thermal Infrared Sensor (TIRS) Level-2 products were acquired for representative months in summer, monsoon, and winter seasons, each with <10% cloud cover. Bands 4, 5, 6, and 10 were used for surface reflectance, vegetation indices, and Land Surface Temperature (LST) derivation.

Land Use/Land Cover (LULC)**:** A high-resolution LULC map was prepared from Sentinel-2 imagery (10 m), classified into categories compatible with the InVEST biophysical table, and validated using field survey points and high-resolution reference imagery.

Biophysical Parameters: Albedo, vegetation fraction, and canopy height values were assigned to each LULC class based on field observations within Pune and literature values, following InVEST guidelines.

Evapotranspiration (ET)**:** Seasonal ET rates were obtained from the MOD16A2 global product (8- day composites, 500 m resolution) and resampled to match the Landsat grid for integration into the model.

Population and Administrative Boundaries: Census 2011 population data and official PMR administrative boundary shapefiles were used for spatial aggregation and reporting.

Validation Data: Ground-based air temperature observations from India Meteorological Department (IMD) stations within PMR were used to cross check LST patterns and provide contextual validation of InVEST model outputs.

All datasets were preprocessed to ensure uniform projection, extent, and spatial resolution, enabling the derivation of seasonal LST composites and subsequent calculation of Cooling Capacity and Heat Mitigation Index (HMI) at 30 m resolution for metropolitan-scale analysis.

3. METHODOLOGY

The methodological framework integrated multisource remote sensing datasets with the InVEST Urban Cooling Model to quantify spatial patterns of Cooling Capacity (CC) and Heat Mitigation Index (HMI) across the Pune Metropolitan Region (PMR). The workflow comprised data acquisition, preprocessing, land surface temperature (LST) retrieval, land use/land cover (LULC) classification, biophysical parameterization, and model execution with ./l.

https://doi.org/10.5194/isprs-annals-X-5-W2-2025-149-2025 | © Author(s) 2025. CC BY 4.0 License.

3.1 Land Surface Temperature Retrieval

Seasonal LST composites were generated from Landsat 8 OLI/TIRS Level-2 imagery representing summer, monsoon, and winter periods, each with <10% cloud cover. Thermal Band 10 was processed through radiometric conversion, atmospheric correction, emissivity adjustment, and conversion to LST, ensuring all physical units were consistent. Multi-scene mosaics were composited for each season to minimize residual cloud and atmospheric effects. The steps were as follows:

1. Conversion of Digital Numbers to Top-of-Atmosphere (TOA) Spectral Radiance:
$L_\lambda = M_L \times Q_{cal} + A_L$ (1)
where L_λ is the TOA spectral radiance ($W \cdot m^{-2} \cdot sr^{-1} \cdot \mu m^{-1}$), M_L is the radiance multiplicative scaling factor, Q_{cal} is the quantized calibrated pixel value, and A_L is the radiance additive scaling factor.

2. Conversion to Brightness Temperature (BT):
$BT = K_2 / \ln(K_1 / L_\lambda + 1)$ (2)
where K_1 and K_2 are thermal conversion constants for Landsat 8 TIRS Band 10, and BT is in Kelvin.

3. Emissivity Estimation from NDVI:
$NDVI = (\rho_{NIR} - \rho_{RED}) / (\rho_{NIR} + \rho_{RED})$ (3)

4.Fractional vegetation cover (PV) was calculated as:
$PV = ((NDVI - NDVI_s) / (NDVIv - NDVI_s))^2$ (4)
where $NDVI_s$ =0.2 and $NDVI_v$ =0.5 are NDVI values of bare soil and full vegetation, respectively.
5.Surface emissivity (ε) was then estimated as: $\varepsilon = 0.004 \times PV + 0.986$ (5)

6. Final LST Calculation:
$LST = BT / (1 + (\lambda \times BT / \rho) \times \ln \varepsilon)$ (6)
where λ is the wavelength of emitted radiance (11.5 μm for Band 10), and $\rho = hc / k = 1.438 \times 10^{-2}$ m·K, with h = Planck's constant, c = speed of light, and k = Boltzmann constant. The LST output is in Kelvin and converted to °C by subtracting 273.15.

3.2 Land Use/Land Cover Classification and Biophysical Parameterization

A supervised classification of Sentinel-2 imagery (10 m) was undertaken using training data from field surveys and high-resolution Google Earth imagery. The classification scheme was harmonized with the InVEST biophysical table, comprising seven major classes: Dense Vegetation, Open Vegetation, Agriculture, Built-up (High Density), Built-up (Low Density), Water Bodies, and Barren Land.

Post-classification accuracy assessment employed an independent validation dataset of 350 ground truth points stratified across all LULC classes. The overall classification accuracy was 87.4% with a Kappa coefficient of 0.82, indicating substantial agreement. Each LULC class was assigned biophysical parameter values (albedo, vegetation fraction, and canopy height) derived entirely from established literature sources for tropical urban environments and InVEST model defaults (Bosch & Hamel, 2021; Kadaverugu & Sharma, 2021; Hamel et al., 2024). Parameter values were selected based on studies from similar climatic regions and validated through comparison with remotely-sensed vegetation indices and surface reflectance characteristics.

3.3 Evapotranspiration Data Integration

Seasonal evapotranspiration rates were sourced from the MOD16A2 global product (8 day composites, 500 m resolution) and bilinearly resampled to the 30 m Landsat grid for model integration. This step ensured spatial alignment of all raster inputs, while preserving the native resolution of the MODIS product in terms of inherent spatial detail.

3.4 Model Parameterization

The InVEST Urban Cooling Model was parameterized using a biophysical table assigning albedo, evapotranspiration, and vegetation/shade values to each LULC class. The biophysical parameters were derived from a combination of field measurements, literature sources, and model defaults as recommended in (Bosch & Hamel, 2021) and (Hamel et al. 2024). Albedo values were estimated from surface reflectance data, while shade coefficients were based on canopy height and vegetation density.

The maximum cooling distance was set to 300 m, following recommendations for medium-density tropical cities (Hasan, 2024; Kadaverugu & Sharma, 2021). Predictor weights for evapotranspiration, shade, and albedo were assigned as 0.4, 0.4, and 0.2**,** respectively, to reflect the relative contribution of each process to cooling capacity. The reference rural air temperature was estimated from IMD station data outside the urban heat island influence zone.

The InVEST Urban Cooling Model estimates Cooling Capacity (CC) as a weighted combination of shade, evapotranspiration, and albedo:
$CC_i = w_s \cdot S_i + w_{ET} \cdot ET_i + w_a \cdot A_i$ (7)
where S_i corresponds to the vegetation/shade fraction values from Table 1, ET_i represents normalized evapotranspiration derived from MOD16A2 seasonal composites (resampled to 30 m resolution), and A_i represents normalized albedo calculated from the albedo values in Table 1. All indices are normalized to a 0-1 scale, with weights ws = 0.4, wET = 0.4, and wa = 0.2.

The Heat Mitigation Index (HMI) was calculated as:
$HMI_i = CC_i / (1 + d_i / d_{max})$ (8)
where d_i is the distance from pixel i to the nearest cooling source, and d_{max} = 300 m is the maximum cooling distance beyond which cooling effects are negligible.

LULC Class	Albedo	Vegetation/ Shade Fraction	Evapo-transpiration (mm/day)	Canopy Height (m)
Dense Vegetation	0.20	0.85	4.5	10
Open Vegetation	0.22	0.65	3.8	5
Agriculture	0.23	0.60	3.5	3
Built-up (High Density)	0.15	0.10	0.8	0
Built-up (Low Density)	0.18	0.25	1.5	0
Water Bodies	0.08	0.00	5.0	0
Barren Land	0.28	0.05	0.5	0

Table 1. Biophysical parameters used for each LULC class

https://doi.org/10.5194/isprs-annals-X-5-W2-2025-149-2025 | © Author(s) 2025. CC BY 4.0 License.

4. RESULTS

4.1 Seasonal Land Surface Temperature Patterns

Seasonal LST composites revealed clear spatial and temporal variations in thermal intensity across the Pune Metropolitan Region (PMR). Summer exhibited the highest mean LST values, particularly in the dense built-up zones of central Pune, Pimpri-Chinchwad, and key transport corridors, while monsoon months displayed the lowest overall LST due to high cloud cover and evapotranspiration rates. Winter values were intermediate, with distinct warm pockets persisting in industrial and commercial districts (Figure 2). Mean seasonal LST ranged from 19.8°C in vegetated peri-urban wards to 41.2°C in industrial brownfield sites during summer.

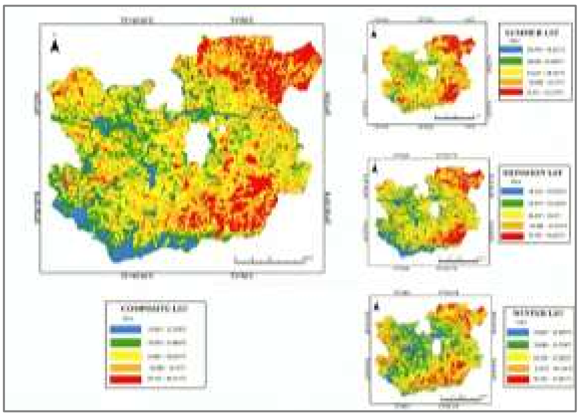

Figure 2. Seasonal LST maps for summer, monsoon, and winter for the Pune Metropolitan Region for 2024

4.2 Cooling Capacity (CC) Distribution

Cooling Capacity (CC) values, computed using the InVEST Urban Cooling Model, exhibited a spatial gradient strongly aligned with vegetation cover and urban morphology. High CC zones (0.69-0.94) corresponded to forested and well-vegetated areas along river corridors, hill slopes, and peri-urban agricultural lands.

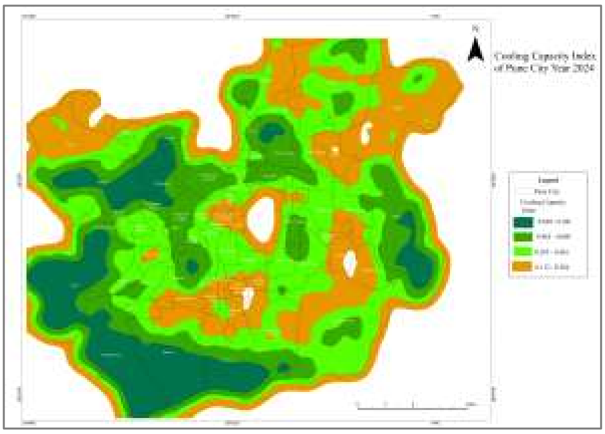

Figure 3. Spatial distribution of Cooling Capacity across the Pune Metropolitan Region

Low CC zones (0.12-0.20) were concentrated in high-density built-up wards, particularly in industrial and commercial clusters (Figure 3). The CC results indicated that even within dense urban areas, localised green spaces and riparian buffers contributed to measurable cooling benefits.

4.3 Heat Mitigation Index (HMI)

HMI values, which integrate CC with spatial proximity to green infrastructure and high LST 'heat source' zones, showed marked spatial clustering. Wards in the city's western and southern peripheries achieved high HMI scores (0.71-0.94), reflecting both high cooling potential and strategic distribution of vegetation. In contrast, the central business districts and industrial belts registered low HMI (0.12-0.33), indicating high vulnerability to UHI effects and low proximity to effective cooling sources (Figure 4).

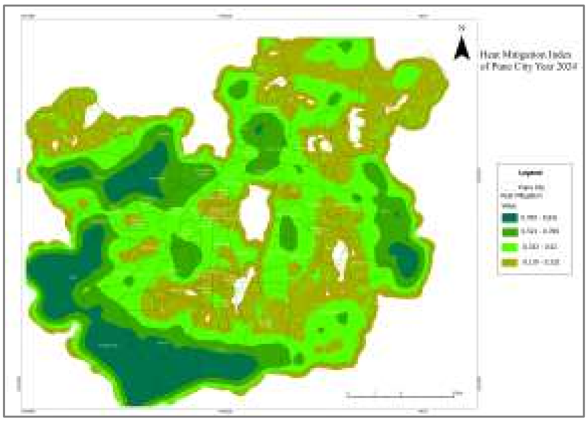

Figure 4. HMI map for Pune Metropolitan Region for 2024

4.4 Seasonal Variations in Cooling Effectiveness

Seasonal comparisons indicated that CC and HMI were highest during the monsoon due to elevated evapotranspiration, moderate during winter, and lowest in summer when vegetation stress and surface dryness reduced cooling performance. Statistical summaries showed that the mean summer CC was 0.41, compared to 0.54 in the monsoon and 0.46 in winter. Mean HMI values followed a similar pattern: 0.39 (summer), 0.53 (monsoon), and 0.44 (winter).

Category	Cooling Capacity Index	Heat Mitigation Index
High	0.685 – 0.943	0.708 – 0.943
Moderate-High	0.475 – 0.684	0.512 – 0.707
Moderate-Low	0.293 – 0.474	0.327 – 0.511
Low	0.116 – 0.202	0.116 – 0.326

Table 2. Seasonal statistics for CC and HMI across the Pune Metropolitan Region (Note: Values represent the full range across all three seasons (summer, monsoon, winter)

These seasonal patterns are clearly visible in the spatial distributions shown in Figures 2-4, where monsoon conditions consistently show higher cooling effectiveness across all land use types. The temporal variations in CC and HMI reflect the seasonal influence of evapotranspiration and vegetation phenology on urban cooling services. The 40%

increase in mean HMI from summer (0.39) to monsoon (0.53) demonstrates the critical role of moisture availability in enhancing cooling capacity. This seasonal pattern was consistent across all LULC classes, with the most pronounced improvements observed in vegetated areas where evapotranspiration rates increased substantially during the monsoon period.

Winter values (CC = 0.46, HMI = 0.44) represented intermediate conditions, with moderate evapotranspiration but reduced vegetation stress compared to summer. The 26% seasonal variation in cooling effectiveness indicates that UHI mitigation strategies should account for monsoon-enhanced cooling when planning intervention timing and expected benefits.

Spatial analysis revealed that areas with high vegetation cover (dense vegetation and open vegetation classes) showed the greatest seasonal variability, with HMI improvements of up to 35% from summer to monsoon, while built-up areas showed minimal seasonal changes (<10% variation), highlighting their consistently poor cooling performance throughout the year.

4.5 Validation

Comparison of modelled HMI-derived temperature reduction with IMD station air temperature data yielded R^2 values of 0.73 for summer, 0.78 for monsoon, and 0.69 for winter, with RMSE ranging from 1.2°C to 1.6°C. These results confirmed that the InVEST Urban Cooling Model adequately captured the spatial variability of cooling services across PMR at a 30 m resolution.

4.6 Priority Areas for Greening Interventions

By overlaying low-HMI zones with socio-economic and land availability data, the study identified priority wards for targeted greening interventions. The prioritization was based on areas exhibiting both high thermal vulnerability (low HMI values in the 0.12–0.33 range) and feasible opportunities for green infrastructure development.

Identified Priority Wards
Four key wards were identified as high-priority areas for greening interventions:
Khadki: Industrial ward with low HMI values and opportunities for workplace greening
Bhosari: Manufacturing zone requiring cooling interventions for worker thermal comfort
Yerawada: Mixed residential-commercial area with limited existing green cover
Kasba Peth: Dense urban core with minimal vegetation and high built-up density

These priority wards collectively represent 22% of PMR's high-vulnerability zones while also exhibiting feasible land availability for implementing urban forests, green roofs, and vegetated corridors.

Intervention Framework
The spatial analysis provides a foundation for stakeholder engagement, enabling municipal authorities, NGOs, and citizen groups to focus greening efforts where cooling benefits would be maximized. The identified areas offer opportunities for:

- Urban forests in available open spaces
- Green roofs on industrial and commercial buildings
- Vegetated corridors along transport routes
- Community gardens in residential neighbourhoods

This targeted approach ensures that limited resources for urban greening are strategically deployed in areas where they can provide the greatest cooling benefits while serving communities most vulnerable to UHI effects.

Community Engagement Pathway: The HMI maps provide accessible visual tools for engaging resident associations, environmental NGOs, and neighbourhood groups in greening initiatives. The spatial prioritization enables community organizations to advocate for targeted interventions in areas where cooling benefits are scientifically demonstrated, supporting evidence-based participatory planning.

Monitoring and Adaptive Management: Follow-up LST and HMI assessments should be conducted 3-5 years post-implementation to evaluate intervention effectiveness and guide adaptive management of the urban cooling network. The established baseline provides a framework for quantifying cooling benefits achieved through community-led and institutional greening efforts.

5. DISCUSSION

The results of this study highlight the significant spatial variability of Cooling Capacity (CC) and Heat Mitigation Index (HMI) across Pune's urban-rural continuum, reflecting both natural vegetation patterns and urban design choices. High CC and HMI values were concentrated in wards with dense vegetation, such as large parks and institutional campuses, consistent with findings from (Favazza et al. 2022, Hasan 2024) who observed similar relationships between vegetation cover and urban cooling. Conversely, low CC and HMI scores in 'brown-zone' wards underscore the role of impervious surfaces in exacerbating Urban Heat Island (UHI) intensity, aligning with Parlow (2021) and Ullah et al. (2025).

The InVEST Urban Cooling Model proved effective in integrating biophysical parameters such as shade, evapotranspiration (ET), and albedo-into a spatially explicit framework that identifies priority areas for greening. The range of CC values in this study (0.72 to 0.28) compares well with other applications. For example, Hasan (2024) reported an HMI range of 0.75 to 0.31 for Rajshahi, Bangladesh, with every 0.1 increase in HMI corresponding to a 0.53 °C drop in LST. Kadaverugu & Sharma (2021) found CC values between 0.70 and 0.25 for Nagpur, India, with scenario analysis predicting up to 1.5 °C surface temperature reduction when high-priority greening zones were implemented. Internationally, Bosch & Hamel (2021) documented HMI ranges from 0.78 to 0.36 in Singapore, linked to mean daytime air temperature reductions of 1.2-1.8 °C, while Hamel et al. (2024) reported that optimally placed vegetation in Paris achieved up to 2.0 °C cooling at local scales. These parallels validate both the methodological approach and the robustness of the Pune results.

5.1 Model Limitations and Uncertainty Assessment

Several limitations and sources of uncertainty should be acknowledged in interpreting these results:

The resampling of MOD16A2 evapotranspiration data from 500 m to 30 m resolution may introduce spatial smoothing effects that could underestimate cooling variability in heterogeneous urban areas. While bilinear resampling preserved general spatial patterns, fine-scale ET variations around individual buildings and small green spaces may not be fully captured.

The three seasonal composites (summer, monsoon, winter) represent mean conditions but do not capture extreme heat events or short-term thermal variations that may be critical for public health impacts. The <10% cloud cover threshold for Landsat scenes may have introduced selection bias toward clearer atmospheric conditions.

The InVEST Urban Cooling Model assumes linear relationships between biophysical parameters and cooling capacity, which may oversimplify complex urban microclimate processes. The fixed 300 m maximum cooling distance, while appropriate for tropical cities, may vary with local topography and wind patterns not explicitly modelled. Biophysical parameters derived entirely from literature sources introduce uncertainty, as local conditions may vary from reference studies. The assigned weights (shade: 0.4, ET: 0.4, albedo: 0.2) reflect general recommendations but local optimization could improve model performance.

6. CONCLUSION

While the MOD16A2 evapotranspiration product resampled to 30 m resolution provided consistent and validated seasonal inputs for this study, future work could explore finer-resolution ET estimation to further enhance spatial detail in CC and HMI outputs. Approaches such as Landsat-based SSEBop or NDVI-derived crop coefficients could capture micro-scale variations in irrigated parks, lakeside green belts, and roadside tree plantations that are not fully resolved at 500 m. Data fusion techniques combining the temporal density of MODIS with the spatial sharpness of Landsat or Sentinel-2 offer promising pathways for producing seamless 30 m ET surfaces. These refinements would be particularly valuable for neighbourhood scale planning and participatory greening initiatives through citizen networks, while maintaining the broader scale comparability afforded by the current MODIS based approach.

The integration of decision ready outputs into the citizen science geo framework enhances their utility beyond academic analysis. By presenting spatial priorities in a format accessible to municipal authorities, NGOs, and resident associations, the maps and indices support participatory decision-making and citizen-led greening initiatives. This aligns with recommendations from Weng (2020) and Cecinati et al. (2019) that remote sensing outputs should be coupled with locally relevant engagement mechanisms to translate science into adaptive governance. In the Pune context, these outputs can inform targeted interventions-such as urban forests, green roofs, and street tree corridors-that are co-designed with community stakeholders to maximise both climate and social benefits.

Overall, the findings demonstrate that coupling geospatial modelling with citizen engagement platforms can translate scientific insights into actionable strategies for climate resilience. This study's integration of UHI analysis, biophysical parameterisation, and participatory planning contributes a replicable model for other rapidly urbanising Indian metropolitan regions, ensuring that geospatial intelligence directly supports community-driven climate adaptation.

7. REFERENCES

Bosch, M., & Hamel, P., 2021. A spatially explicit approach to simulate urban heat mitigation with InVEST (v3.8.0). *Geosci. Model Dev.*, 14, 3521–3539. https://doi.org/10.5194/gmd-14-3521-2021

Cecinati, F., Amitrano, D., Leoncio, L. B., Walugendo, E., Guida, R., Iervolino, P., & Natarajan, S., 2019. Exploitation of ESA and NASA heritage remote sensing data for monitoring the heat island evolution in Chennai with the Google Earth Engine. *Int. Geosci. Remote Sens. Symp.*, 8898040. https://doi.org/10.1109/IGARSS.2019.8898040

Duan, H., Haseeb, M., Tahir, M., Mahmood, S., Tariq, S., Jamil, U., Ullah, I., & Abdullah-Al-Wadud, M., 2025. A geospatial and statistical analysis of land surface temperature in response to land use land cover changes and urban heat island dynamics. *Sci. Rep.*, 15, 89167. https://doi.org/10.1038/s41598-025-89167-x

Elmarakby, A., & Elkadi, H., 2024. Prioritising urban heat island mitigation interventions: Mapping a heat risk index. *Sci. Total Environ.*, 174927. https://doi.org/10.1016/j.scitotenv.2024.174927

Favazza, F., Gagliano, A., Mangiameli, M., & Mussumeci, G., 2022. Remote sensing to analyse Urban Heating Island. A case study from Catania (Sicily). *Nucleation and Atmospheric Aerosols*. https://doi.org/10.1063/5.0081747

Hamel, P., Bosch, M., & Tardieu, L., 2024. Calibrating and validating the Integrated Valuation of Ecosystem Services and Tradeoffs (InVEST) urban cooling model: Case studies in France and the United States. *Geosci. Model Dev.*, 17, 4755–4772. https://doi.org/10.5194/gmd-17-4755-2024

Hamel, P., & Bosch, M., 2023. Calibrating and validating the InVEST urban cooling model: Case studies in France and the United States. *EGUsphere*. https://doi.org/10.5194/egusphere-2023-928

Hasan, J., 2024. Evaluating the impact of green spaces on urban heat reduction in Rajshahi, Bangladesh using the InVEST model. *Land*, 13(8), 1284. https://doi.org/10.3390/land13081284

Isinkaralar, Y., Yeboah, G., Isinkaralar, T., Sarfo, I., Öztürk, Y., Yilmaz, E., & Bojago, E., 2025. Investigating the effects of local climate zones on land surface temperature using spectral indices via linear regression model: A seasonal study of Sapanca Lake. *Environ. Monit. Assess.*, 197, 13705. https://doi.org/10.1007/s10661-025-13705-3

Kadaverugu, R., & Sharma, A., 2021. Quantification of heat mitigation by urban green spaces using InVEST model—a scenario analysis of Nagpur City, India. *Arab. J. Geosci.*, 14, 1218. https://doi.org/10.1007/s12517-020-06380-w

Korotczuk-Zych, M., 2023. Planning of urban greenspace for cooling Singapore: Modeling the cooling effects of greenspace and urban morphology. *EGUsphere*. https://doi.org/10.5194/egusphere-egu23-11790

Li, F., Yiğitcanlar, T., Nepal, M. P., Nguyen, K., & Dur, F., 2024. A novel urban heat vulnerability analysis: Integrating machine learning and remote sensing for enhanced insights. *Remote Sens.*, 16(16), 3032. https://doi.org/10.3390/rs16163032

Parlow, E., 2021. Regarding some pitfalls in urban heat island studies using remote sensing technology. *Remote Sens.*, 13(18), 3598. https://doi.org/10.3390/rs13183598

Saini, R., Gupta, A., Dhupper, V., & Shrivastava, P., 2025. Spatio-temporal study of urban dynamics with implications on land surface temperature of Gurugram City, India. *Environ. Monit. Assess.*, 197, 14392. https://doi.org/10.1007/s10661-025-14392-w

Soto, D., Nedjai, R., Selouane, K., & Ziv, N., 2023. On the use of remote sensing and modeling techniques for urban heat detection, an operational study. *Joint Urban Remote Sensing Event*. https://doi.org/10.1109/JURSE57346.2023.10144167

Ullah, I., Qiao, J., & Tariq, S., 2025. Impact assessment of planned and unplanned urbanization on land surface temperature in Afghanistan using machine learning algorithms: A path toward sustainability. *Sci. Rep.*, 15, 87234. https://doi.org/10.1038/s41598-025-87234-x

Weng, Q., 2020. Urban heat islands modeling and analysis. In *IEEE Xplore*. https://doi.org/10.1002/9781119307303.CH6

Xu, C., Huang, Q., Haase, D., Dong, Q., Teng, Y., Su, M., & Yang, Z., 2024. Cooling effect of green spaces on urban heat island in a Chinese megacity: Increasing coverage versus optimizing spatial distribution. *Environ. Sci. Technol.*, 58(4), 2345–2358. https://doi.org/10.1021/acs.est.3c11048

Zardo, L., Geneletti, D., Pérez-Soba, M., & Van Eupen, M., 2017. Estimating the cooling capacity of green infrastructure for urban planning: A case study in the Netherlands. *Landsc. Urban Plan.*, 159, 85–97. https://doi.org/10.1016/j.landurbplan.2016.11.012